Atmos. Chem. Phys., 15, 1621–1632, 2015
www.atmos-chem-phys.net/15/1621/2015/
doi:10.5194/acp-15-1621-2015

Atmospheric Chemistry and Physics
Open Access

Deposition-mode ice nucleation reexamined at temperatures below 200 K

E. S. Thomson[1], X. Kong[1], P. Papagiannakopoulos[1,2], and J. B. C. Pettersson[1]

[1]Department of Chemistry and Molecular Biology, Atmospheric Science, University of Gothenburg, 412 96, Gothenburg, Sweden
[2]Laboratory of Photochemistry and Kinetics, Department of Chemistry, University of Crete, 71003 Heraklion, Crete, Greece

Correspondence to: E. S. Thomson (erik.thomson@chem.gu.se) and J. B. C. Pettersson (janp@chem.gu.se)

Received: 2 July 2014 – Published in Atmos. Chem. Phys. Discuss.: 15 September 2014
Revised: 27 December 2014 – Accepted: 15 January 2015 – Published: 16 February 2015

Abstract. The environmental chamber of a molecular beam apparatus is used to study deposition nucleation of ice on graphite, alcohols and acetic and nitric acids at temperatures between 155 and 200 K. The critical supersaturations necessary to spontaneously nucleate water ice on six different substrate materials are observed to occur at higher supersaturations than are theoretically predicted. This contradictory result motivates more careful examination of the experimental conditions and the underlying basis of the current theories. An analysis based on classical nucleation theory supports the view that at these temperatures nucleation is primarily controlled by the rarification of the vapor and the strength of water's interaction with the substrate surface. The technique enables a careful probing of the underlying processes of ice nucleation and the substrate materials of study. The findings are relevant to atmospheric nucleation processes that are intrinsically linked to cold cloud formation and lifetime.

1 Introduction

In the atmosphere water vapor is transformed into cloud particles and precipitation vis-á-vis processes of nucleation, whereby vapor becomes liquid droplets or solid ice particles. The nucleation and evolution of droplets and ice crystals is a keystone process for both the global radiative balance and the hydrologic cycle. In most of the atmospheric column the temperature and saturation conditions dictate that solid ice is the thermodynamically favorable phase. However, in the real world, spontaneous ice formation is difficult to achieve and fundamentally quantifying atmospheric ice nucleation and growth remains an elusive scientific goal. The processes of ice nucleation are invariably influenced by the presence of other atmospheric constituents like particles and/or gases, meaning that the nucleation that is observed to be important in the atmosphere is largely heterogeneous. Heterogeneous *ice* nucleation may occur when (1) supercooled liquid water contacts a foreign body and subsequently freezes, or (2) when H_2O vapor is directly deposited onto foreign material (Pruppacher and Klett, 1997). The later mechanism, also referred to as *deposition freezing*, is an important mechanism of ice formation at low atmospheric temperatures. Like other freezing mechanisms (e.g., immersion-mode freezing, Marcolli et al., 2007; Möhler et al., 2005), measurements of deposition freezing show wide ranges of nucleation onset (Knopf and Koop, 2006; Möhler et al., 2006) and assessing the relative importance of different freezing modes remains an active area of inquiry (Hoose and Möhler, 2012), most critically at high temperatures and near water saturation where multiple freezing mechanisms may be active (Dymarska et al., 2006). That said, at low temperatures, deposition freezing experiments are relatively straightforward and therefore provide an excellent template for detailed comparisons of observation and theory.

The fundamental character of nucleation as a statistical thermo-kinetic process makes it difficult to achieve an unambiguous mathematically predictive nucleation theory. Modeling nucleation is made difficult by the challenge of capturing the scope of nucleating systems; from molecular clustering to macroscopically observed solidification, and the observational barriers to detecting nucleation onset, efficiency,

and particle growth rates (Fletcher, 1958; Hale and Plummer, 1974; Kashchiev, 2006). However, due to the fundamental importance of nucleation to phase behavior, much attention is paid to extracting and appraising the relevant kinetic and thermodynamic parameters (Chen et al., 2008; Liu, 1999; Niedermeier et al., 2011). For atmospheric ice nucleation the impediments to understanding are particularly formidable. Environmental temperature and saturation conditions, and the time and turbulent scales of the atmosphere are difficult to simulate in a laboratory. Field campaigns that yield spatially and temporally resolved free troposphere data are also difficult and resource intensive. Obstacles aside the current escalation of interest in atmospheric ice nucleation is and needs to be driven towards formulating true microphysical understanding that can be used in describing clouds and other atmospheric processes.

Low-temperature deposition nucleation experiments are relatively straight forward to execute in a laboratory setting using idealized substrate surfaces and the results can be applied to assessing the validity of ice nucleation parameterizations that seek to illuminate atmospheric processes. Here we describe a series of deposition ice nucleation experiments at temperatures ≤ 200 K, where our initially surprising results share commonality with previously measured deposition nucleation on minerals (Fortin et al., 2003; Trainer et al., 2009), metals (Shilling et al., 2006), and other materials (Iraci et al., 2010; Phebus et al., 2011; Cziczo et al., 2013). Our measurements augment the observations of nucleation behavior at low temperature and have led us to reexamine the classical formulation of nucleation theory. This examination has motivated us to probe the microphysics of nucleation at these temperatures and forces us to investigate what limits small ice embryo formation at low temperature. This makes plain the need for renewed investigation into the microphysics of nucleation and is important for understanding the formation of small surface water clusters and the behavior of a range of ice nucleating materials.

2 Experimental

2.1 Apparatus

These experiments utilize an Environmental Molecular Beam (EMB) chamber contained within a multi-chamber ultra-high vacuum (UHV) system that has been described previously (Kong et al., 2011 and Fig. 1). Within the environmental chamber highly oriented pyrolytic graphite (HOPG, produced by Advanced Ceramics Corp., grade ZYB) is utilized as a bare substrate and a surface upon which other molecular materials can be condensed. The 12 mm × 12 mm surface is temperature controlled and gas inlets are positioned to facilitate the introduction of condensing species like water that form layers on the HOPG. Helium in the molecular beam provides a sensitive measure of nucleation on, and coverage of, the graphite surface (Kong et al., 2012). Macroscopic thickness, ice nucleation and growth, are also monitored from the reflected intensity of a 0.86 mW, 670 nm diode laser. A quadrupole mass spectrometer (QMS) is positioned within the primary UHV chamber in line with an opening in the environmental chamber. Thus, the QMS provides a sensitive measure of the environmental chamber pressure and the molecular species leaving the cold HOPG surface.

When investigating critical supersaturations for ice nucleation the experimental procedure begins by setting the surface temperature T_s (Kong et al., 2012). The graphite is then used as a bare surface or as a cold surface for condensing substrate materials of interest. Here we present results of ice nucleation on bare graphite and adlayers of methanol (MeOH), butanol (BuOH), hexanol (HxOH), acetic acid (AcOH) and nitric acid (HNO_3). For each condensed material, prior to inletting water vapor to induce nucleation, a stable substrate monolayer is adsorbed onto the graphite. On graphite monolayers of these materials are significantly more stable than equivalent macroscopic layers, and using the EMB can be characterized by adsorption isotherms determined from helium scattering (Kong et al., 2012; Papagiannakopoulos et al., 2014). The QMS is used to measure the water vapor intensity $\mathcal{I}_{bk}, \mathcal{I}_{nuc}, \mathcal{I}_{eq}$, where the subscripts refer to the states of the system (bk – background, nuc – nucleation, or eq – equilibrium). In this case the measured intensities directly represent the physical parameter of interest, pressure $P \propto \mathcal{I}_{bk}, \mathcal{I}_{nuc}, \mathcal{I}_{eq}$. After a background intensity $\mathcal{I}_{bk}$ is identified, water vapor is systematically added to the system until ice nucleation is observed. Typically experimental time scales to reach the critical saturation for nucleation S_i^{nuc} are on the order of 10 to 15 min. Vapor is initially inlet to an estimated level of $0.9S_i^{nuc}$, and after the system has re-equilibrated at that level small incremental increases are made in H_2O vapor pressure at one minute intervals. The H_2O intensity required for ice nucleation $\mathcal{I}_{nuc}$ is recorded and subsequently the ice layer is grown to a macroscopic thickness of $\approx 1\,\mu$m. After achieving a macroscopic ice layer the vapor inlet is adjusted to maintain a constant, homogeneous ice layer in near equilibrium with the vapor and the steady-state vapor pressure over the ice $\mathcal{I}_{eq}$ is measured. Thus, at each temperature all relevant vapor pressures are explicitly measured and the critical supersaturation required for ice nucleation can be calculated directly as described in Sect. 2.2.

2.2 Results

The direct linear relationship between the pressure within the environmental chamber and the intensity measured with the QMS, allows us to calculate the chamber supersaturations at the onset of nucleation. The range of temperature that we are able to explore using this method ($155\,\text{K} \leq T_s \leq 200\,\text{K}$) extends from the temperature at which the chamber background pressure exceeds S_i^{nuc} to the highest T_s at which an equilibrium ice surface is sensitive to the inlet vapor flux. At

temperatures greater than 200 K the vapor inlet valve must be fully open to maintain equilibrium ice surfaces, which limits experimental control and precludes accurate pressure measurements.

The critical supersaturation for nucleation is defined as the ratio of the nucleation vapor pressure to the equilibrium vapor pressure above the condensed phase. Expressed in terms of the measured QMS intensities, after the chamber's background intensity is carefully removed, yields

$$S_{\mathrm{i}}^{\mathrm{nuc}} = \frac{\mathcal{I}_{\mathrm{nuc}}}{\mathcal{I}_{\mathrm{eq}}}. \quad (1)$$

This straightforward analysis was observed to be robust for all of the measured systems with the exception of the extreme temperatures measured for the pure ice on graphite nucleation. For that system at $T_{\mathrm{s}} \geq 195\,\mathrm{K}$, $\mathcal{I}_{\mathrm{eq}}$ was observed to be affected by the high absolute vapor pressures. The high absolute pressures were observed to stress the UHV pumping capacity and therefore shift the background intensity. The shift was calculated by comparing the $T_{\mathrm{s}} \geq 195\,\mathrm{K}$ to expected results based on a Clausius–Clapyron fitting of the lower temperature data and used as a small correction to the data. The corrected results compare well with the independent results of Pratte et al. (2006). Likewise for graphite at $T_{\mathrm{s}} \leq 160\,\mathrm{K}$, the signal to noise ratio of the measured $\mathcal{I}_{\mathrm{eq}}$ was nearly unity, forcing the results to be corrected based on higher temperature data. For all other substrate materials, tuning the QMS control parameters increased the relative signal, thus allowing the experimentally measured data to be used directly over the entire range of temperature. The results of all measurements are presented in Fig. 2.

In Fig. 2 the critical supersaturations measured for vapor deposition ice nucleation on MeOH, BuOH, HxOH, AcOH, and HNO_3 adlayers, and bare graphite are plotted together with common theoretical curves. For all experimental measurements a strong increase in $S_{\mathrm{i}}^{\mathrm{nuc}}$ is observed with decreasing temperature. The theoretical curves for homogeneous ice nucleation from solution (dashed, Koop et al., 2000, with $J = 5 \times 10^8\,\mathrm{cm}^{-3}\,\mathrm{s}^{-1}$), water saturation (solid black, Murphy and Koop, 2005) and gas phase homogeneous ice nucleation (upper-solid green, Murray and Jensen, 2010) are also drawn. The two former curves, which are both based on low-temperature extrapolations of liquid water properties have been widely used as references for discussing atmospheric ice nucleating processes (e.g., Hoose and Möhler, 2012), and generally it is assumed due to the energetic benefit of surfaces heterogeneous nucleation should occur at or below liquid saturation. However, comparing these curves with the measured values clearly has interesting ramifications. The supersaturations required for ice nucleation are high relative to the theoretical predictions based on liquid parameterizations, and the effect appears to increase exponentially with decreasing temperature – in a manner that appears more consistent with homogeneous nucleation from the gas phase. However, even when the effect is most pronounced,

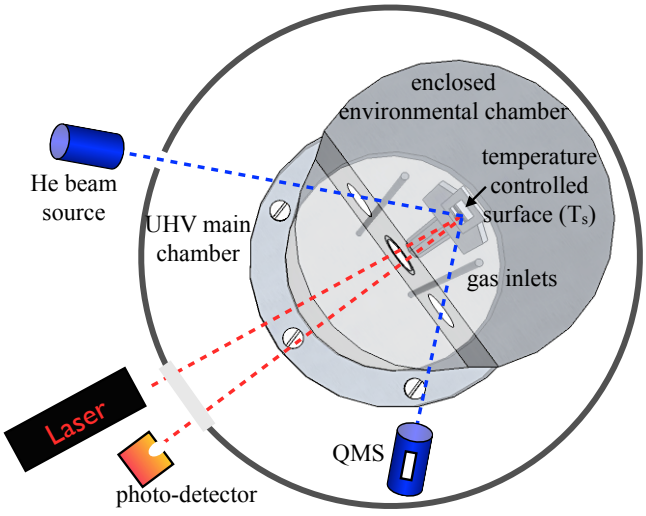

Figure 1. Schematic drawing of the principle components of the environmental chamber and nucleation and growth monitoring system.

Table 1. Shift constants that minimize the cumulative deviation of substrate observations to the homogeneous reference state. Alternatively for each temperature and substrate, this can be expressed mathematically as $\min[\sum(\ln S_{\mathrm{i}}^{\mathrm{nuc}} - \ln S_{\mathrm{i,hom}}^{\mathrm{nuc}})]$, where $\ln S_{\mathrm{i,hom}}^{\mathrm{nuc}}$ represents homogeneous nucleation from the gas phase (green line, Fig. 3).

Surface	Shift constant
Graphite	2.58
Methanol	2.99
Butanol	3.01
Acetic acid	2.71
Hexanol	2.78
Nitric acid	3.19

such as on graphite where $S_{\mathrm{i}}^{\mathrm{nuc}}$ has increased by one order of magnitude at 155 K, the $S_{\mathrm{i}}^{\mathrm{nuc}}$ are significantly enhanced relative to the prediction for homogeneous nucleation. Furthermore, the effect on nucleation is distinguishable between the individual surfaces, making it clear that the specific heterogeneity of each system does play a role.

Although, in absolute terms the onset of nucleation is observed to vary depending on substrate material, Fig. 3 where the data are replotted using an Arrhenius-type formulation illustrates that the trend with temperature is well represented by homogeneous nucleation theory. In Fig. 3 the data from Fig. 2 are re-rendered by taking the logarithm of $S_{\mathrm{i}}^{\mathrm{nuc}}$ and plotting those values vs. inverse temperature. For comparison, the data for each substrate are shifted by a single constant that is chosen to minimize the cumulative deviation from the theoretical curve for homogeneous nucleation (green line). The shift constants are listed in Table 1.

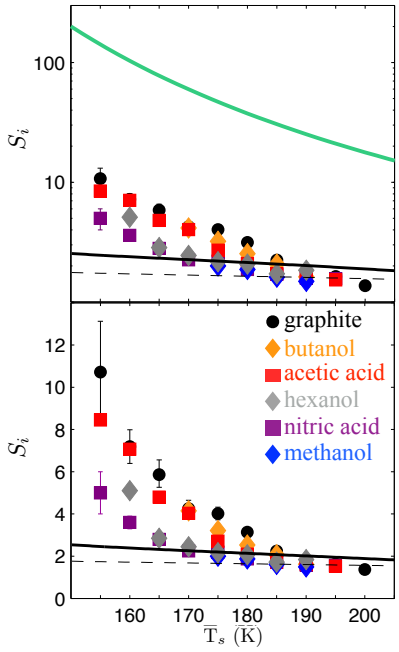

Figure 2. Ice supersaturations (S_i) plotted vs. surface temperature (T_s) with points indicating the critical supersaturations (S_i^{nuc}) required for vapor deposition ice nucleation on various materials. Error limits that are representative of all data are shown for the bare graphite and HNO_3 covered graphite. At $T_s > 165$ K the uncertainty is subsumed by the symbols. For comparison the theoretical curves for water saturation (solid-black, Murphy and Koop, 2005) and homogeneous ice nucleation from solution (dashed, Koop et al., 2000) are also plotted. For the latter a nucleation rate $J = 5 \times 10^8$ cm^{-3} s^{-1} that matches previous treatments (Hoose and Möhler, 2012) is modeled. The logarithmic vertical scale of the upper panel also allows the curve for homogeneous nucleation from the gas phase to be plotted (solid-green, Murray and Jensen, 2010).

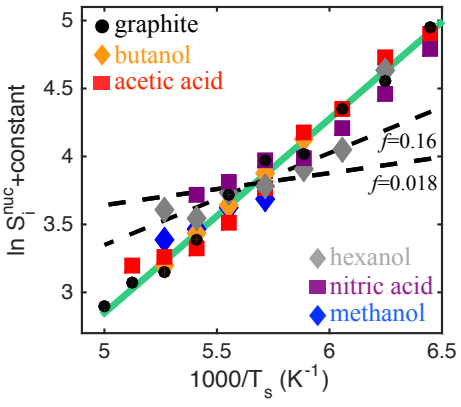

Figure 3. The logarithm of measured critical ice supersaturations S_i^{nuc} plotted vs. inverse temperature. For the purposes of comparison the nucleation data from the different materials are shifted and overlaid with the homogeneous reference case (solid-green line, as in Fig. 2). Although in each case the magnitude of the shift is different, the shifted data all exhibit a temperature trend like that of homogeneous nucleation. Contrastingly, the dashed lines $f = 0.018$ and $f = 0.16$, which represent the extrema of heterogeneous CNT solutions plotted in Fig. 5 and are also shifted and overlaid, do not readily capture the observed temperature trends. Although, the trend with temperature is best captured by the homogeneous theory, the observation of systematic changes in nucleation onset, suggests an underlying dependence on substrate material.

The observation of the homogeneous-like temperature trends in the presence of seemingly high supersaturation values leads us to revisit both classical nucleation theory and our basic understanding of how ice embryos are formed on surfaces.

3 Analysis

Unto themselves the measured S_i^{nuc} values are not completely anomalous. In the past such values have been measured in other systems (Trainer et al., 2009; Fortin et al., 2003; Shilling et al., 2006) and hypothesized as a potential explanation for the absence of ice particles in planetary atmospheres (Iraci et al., 2010). However, past attempts at explaining the few observations have had limited broad applicability, as they often rely on physical parameterizations specific to the investigated systems. The observations we have described augment existing observations and demonstrate the need for a generalized description of deposition nucleation at low temperatures. It is rather unlikely that all observations can be explained by changes in contact angle, site-specific nucleation, or other empirical parameterizations that lack unambiguous chemical or physical explanations at low temperature. For example, in the temperature range of this study graphite is well known to be hydrophobic (Andersson et al., 2007; Kong et al., 2012), while adsorption of methanol provides sites for efficient hydrogen bonding, resulting in a highly hydrophilic surface (Thomson et al., 2011; Kong et al., 2012). Thus, the question remains: how can surfaces with widely dissimilar hygroscopic behavior all require high supersaturations for vapor deposition ice nucleation? To offer insight, we first reexamine the basic edifice of nucleation theory.

3.1 Predicting freezing behavior at low temperature

The nucleation of ice has classically been treated using bulk thermodynamic theories of homogeneous and heterogeneous nucleation. Generally this "classical nucleation theory" (CNT) is flexible enough that it can be used to robustly capture the freezing behavior of many materials including ice. From an analytical point of view the flexibility of CNT stems directly from its mathematical construct,

$$J = A \exp\left(\frac{-\Delta G^*}{k_b T}\right), \quad (2)$$

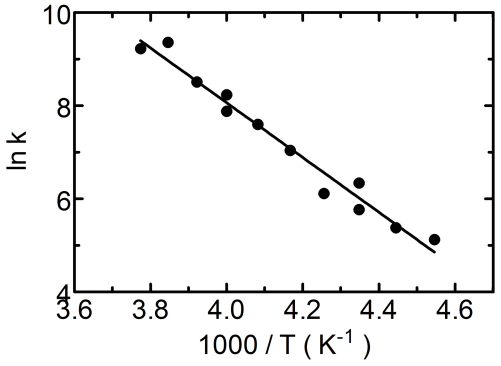

Figure 4. Plot of the logarithm of the desorption rate constant k vs. inverse temperature for D_2O desorbing from HNO_3 monolayers. A linear least squares Arrhenius fitting of the data yields a binding energy of 0.51 ± 0.06 eV with a pre-exponential factor $1 \times 10^{13.7 \pm 1.3}$ indicative of ordinary desorption. The temperature range of the desorption experiments 220 K to 265 K was chosen for experimental accessibility. At $T_S \leq 220$ K the desorption process was too slow to be observed within the experimental time window. However, HNO_3 monolayers on graphite are observed to be very robust with increasing temperature, and thus the water binding energetics are not expected to change. Kong et al. (2014) includes a detailed discussion of D_2O scattering experiments from HNO_3 surfaces.

where the product of a pre-exponential term A and an exponential term that expresses the barrier to nucleation in terms of the free energy of formation of a critical nucleus ΔG^*, Boltzmann's constant k_b and the temperature T, is a nucleation rate J per second per unit volume or area depending upon whether the nucleation occurs in a volume or on a surface. Thus, in its simplest form nucleation is described by a thermodynamic model with an activation barrier. However, as is typical the devil is in the details and much of CNT focuses on the details of the terms ΔG^* and A.

The standard derivation of ΔG^* begins with the surface/volume balance of the free energy of formation of an ice embryo:

$$\Delta G = -V_i \Delta g_v + A_i \gamma, \tag{3}$$

where the volume V_i and area A_i of a spherical ice embryo with radius r_i are $4/3\pi r_i^3$ and $4\pi r_i^2$ respectively, $\Delta g_v = k_b T \ln S/v$ is the bulk energy change per unit volume v expressed in terms of H_2O supersaturation S, and γ is the surface energy of the embryo. Thus, the radius of a critical ice embryo r_i^* is defined as r_i, where $\partial \Delta G/\partial r_i = 0$, or

$$r_i^* = \frac{2\gamma v}{k_b T \ln S}. \tag{4}$$

By substitution this yields a free energy of formation for a homogeneous spherical critical cluster,

$$\Delta G^* = \frac{16\pi \gamma^3 v^2}{3(k_b T \ln S)^2}. \tag{5}$$

In the case of heterogeneous nucleation, when nucleation is facilitated by a foreign material surface, this term can be altered due to the shift in geometry and the change in surface energy caused by the presence of the foreign material. Elegant solutions that depend on the geometry and wettability of the surface–embryo contact have been derived for these considerations and can most simply be expressed as a single factor f that multiplies ΔG^* and can vary from $f = 0$ to $f = 1$ (Pruppacher and Klett, 1997). The result is that the free energy barrier to nucleation is easily scaled and a number of studies have used this to implement contact angle parameterizations that provide suitable statistical fits to experimental data (Chen et al., 2008; Niedermeier et al., 2011). Alternatively, if f is used as a fitting parameter and considered to represent a classical physical contact angle in the Young–Dupre sense the angle and therefore the "wettabilty" of the surface can be determined (Chen et al., 2008). Although surface energy and water contact angle do depend on material, temperature and pressure etc., this method of interpreting measurement data is problematic on several fronts. First, the variation in f that is required to fit experimental data is quite often significant even within small temperature ranges (Trainer et al., 2009). Thus, to achieve a successful CNT fit, a functional dependence of f is often assumed (e.g., Chen et al., 2008; Trainer et al., 2009). These functional dependencies are difficult to verify because at low temperatures and for many materials, the temperature dependence of surface energy and/or contact angle is not independently constrained. Furthermore, the contact angle model is derived based on the assumption of an isotropic spherical ice/water cap. Ice germs are neither isotropic nor necessarily spherical and, at low temperatures, critical sizes on molecular scales may limit the applicability of bulk thermodynamic theories in general. Notwithstanding the fact that contact angle is a useful parameterization, particularly as temperatures approach bulk coexistence, it is plain that it is an empirical parameter and not strictly a physical quantity.

The precise constitution of the pre-exponential term A is also debated, but it is clear that this term represents the molecular fluxes to and from growing embryos. In early work this kinetic coefficient was considered to be an empirically derived constant (e.g., $10^{25}\,s^{-1}\,cm^{-2}$, Fletcher, 1958) to which many processes were shown to be rather insensitive over a few orders of magnitude. Again, at low temperatures, such a treatment of A is problematic and an extra effort must be made to model the active physical processes. In the case of heterogeneous deposition freezing a more descriptive prefactor $A = \alpha\beta\mathcal{Z}N_{ads}$ is often used, where β represents the impingement rate of H_2O molecules onto the critical embryo, $\mathcal{Z}$ is the Zeldovich factor, N_{ads} is the number of adsorbate molecules on the surface, and α represents additional kinetic factors. As given by Winkler et al. (2008), Chen et al. (2008)

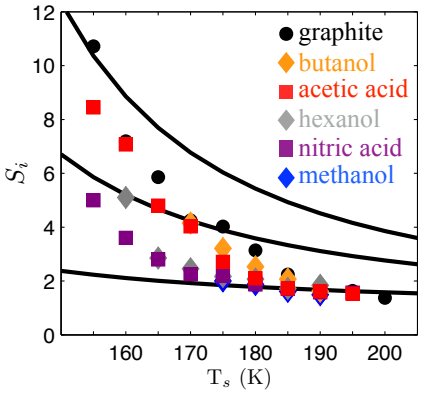

Figure 5. Measurement data plotted similarly to Fig. 2 overlaid with CNT solutions for graphite ($E_{ads} = 0.13$ eV) that assume constant f parameters for the full range of temperature. $f = 0.018, 0.09, 0.16$ (contact angle $\theta \approx 33°$, 51°, 61°) for the lower, middle, and upper curves respectively.

and others,

$$\beta = \frac{S p_s}{\sqrt{2\pi m k_b T}}, \mathcal{Z} = \frac{v}{2\pi r_i^2}\sqrt{\frac{\gamma}{k_b T}},$$
$$N_{ads} = \frac{S p_s}{v\sqrt{2\pi m k_b T}} \exp\left(\frac{E_{ads}}{k_b T}\right), \quad (6)$$

where p_s is the saturation vapor pressure, m and v are the molecular mass and volume, ν is the vibrational frequency of an adsorbed molecule ($10^{13}\,s^{-1}$, Pruppacher and Klett, 1997), and E_{ads} is the adsorption energy of molecules on the surface. Thus, the terms combine to describe the availability of seed molecules on the surface vis-á-vis the balance between monomer adsorption and desorption (N_{ads}), the deposition rate onto growing clusters (β), and a correction factor for the fluctuations that result in some critical clusters returning to sub-critical sizes ($\mathcal{Z}$).

A further oversight at low temperature that comes about due to the classical assumption of bulk properties, is the existence of a finite difference in chemical potential between monomers in the condensed and gaseous phases. By inspection of Eqs. (2)–(5) one can see that the monomer formation energy will be greater than zero, which violates the basic edifice of phase equilibrium. Girshick and Chiu (1990) addressed this specific issue and to insure self-consistency calculated an additional pre-factor,

$$\frac{\exp(\Theta)}{S}, \text{where } \Theta = \frac{\varphi_s \gamma}{k_b T}, \quad (7)$$

that must be incorporated into α. The shape factor $\varphi_s = (36\pi)^{1/3} v^{2/3}$ renders the surface energy dimensionless, and because we are considering the monomer is unaffected by heterogeneity (Kashchiev, 2000).

Thus, combining Eqs. (2)–(7) for the case of heterogeneous nucleation yields a complete expression for the nucleation rate per unit area.

$$J = \frac{\exp(\Theta)}{S} \beta \mathcal{Z} N_{ads} \exp\left(\frac{-\Delta G^*}{k_b T} \times f\right). \quad (8)$$

To utilize this theoretical expression for comparison with the experimental measurements a relevant nucleation rate must be determined. For consistency with other theoretical studies a value of $J = 1\,cm^{-2}\,s^{-1}$ is used (Pruppacher and Klett, 1997; Hoose et al., 2010), but it can also be noted that even order of magnitude changes to the assumed value of J have little effect on results. The adsorption energy E_{ads} within the pre exponential term is the energy that binds molecules to the substrate surface and thus, simply put, the entire exponential pre-factor term summarizes how easy/difficult it is to put and keep molecules on the surface. The values for E_{ads}, which are often not made explicit in the literature are the interaction energies between the H_2O monomer and the substrate surface; and the best values for the experimental substrates used here are listed in Table 2.

3.2 Binding energies

The systems that we have investigated are unique in that they involve monolayer coverages on smooth graphite surfaces. Such molecularly thin coverages necessarily have very different bond arrangements than would their macroscopic counterparts. As a result constraining the appropriate binding energy values presented in Table 2 is difficult and while the numbers presented herein represent the best available values, their provenance does warrant discussion.

Graphite is generally a well characterized material and in the context of this study, has well constrained water interaction energies. The values of H_2O binding energies with graphite are principally constrained by molecular simulations and thus a finite range of values exists that is based on the detail of simulated interaction potentials. However, in general there is close agreement between multiple studies (Marković et al., 1999; Rubeš et al., 2009; Lakhlifi and Killingbeck, 2010; Voloshina et al., 2011). In the case of MeOH, the data reported in Thomson et al. (2011) are affected by complex kinetics in the surface layer that likely involve at least two states with different binding energies. Recalculated binding energies based on a typical Arrhenius prefactor $10^{13}\,s^{-1}$ yield the range of MeOH binding energies presented in Table 2. In a recent study in which BuOH surfaces were investigated in detail, Papagiannakopoulos et al. (2013) used molecular dynamics (MD) simulations to show that water molecules that are able to locate and interact with hydroxyl groups have binding energies between 0.32 and 0.35 eV, but otherwise the interaction is somewhat weaker, 0.10 to 0.12 eV. Complementary EMB–BuOH experiments were consistent with BuOH having a close packed surface structure that precludes the chance for water binding (Papagiannakopoulos et al., 2013). Thus, we suspect the lower values are the best approximation for the monolayers of butanol

Table 2. Surface binding energies.

Surface	Binding energy (eV)	Reference
Graphite	0.10–0.16	Marković et al. (1999); Rubeš et al. (2009); Lakhlifi and Killingbeck (2010); Voloshina et al. (2011)
Methanol	0.37–0.38	Thomson et al. (2011)
Butanol	0.10–0.12	Papagiannakopoulos et al. (2013)
Acetic acid	0.13–0.20	Allouche and Bahr (2006); Papagiannakopoulos et al. (2014)
Hexanol	0.10–0.12 or 0.32–0.35	see Sect. 3.2
Nitric acid	0.51 ± 0.06	Kong et al. (2014) and present study

used in this study, which are expected to have a well-ordered close packed structure. Similar MD simulations do not exist for HxOH and with the present experimental system it is impossible to distinguish the expected H_2O binding energy with a HxOH monolayer from that of BuOH. However, as the alkyl tail elongates it may become more difficult for the layer to relax into its most stable structure and thus it is harder to assess the likelihood that the surface structures will be close packed. The result may be that more OH groups remain available for water binding. The EMB has also been used to study AcOH layers and the experimental results indicate that within a monolayer AcOH–AcOH bonds are strong and it is unlikely that adsorbed water molecules will induce bond breaking. On such surfaces water has a short residence time that effectively sets an upper bound for the H_2O binding energy ≤ 0.25 eV. This agrees with published simulations of water interactions with AcOH hydrophobic surfaces that yield a range of 0.13 to 0.20 eV (Allouche and Bahr, 2006).

The expected water interaction with HNO_3 under our experimental conditions is perhaps the most difficult value to constrain and published binding energy values for water on HNO_3 surfaces are limited. Kołaski et al. (2011) found a value of ≈ 0.35 eV for a H_2O–HNO_3 dimer structure with efficient hydrogen bonding. That is close to the 0.31–0.32 eV determined from ab initio calculations that estimated the formation of stable cyclic monohydrate HNO_3–H_2O complexes (Tao et al., 1996; Staikova and Donaldson, 2001). Our own EMB observations that were complementary to the supersaturation experiments suggest more strongly bound surface states with multiple hydrogen bonds. An Arrhenius plot of data from D_2O scattering from HNO_3 monolayers (Fig. 4) yields the binding energy 0.51 ± 0.06 eV listed in Table 2 and used in our calculations.

It is worthwhile noting that even with the limited number of substances studied here, we do observe a correlation between the binding energy (Table 2) and the absolute shifts (Table 1) required to collapse the data in Fig. 3. Of course this is also seen directly, as the binding energy increases S_i^{nuc} tends to decrease, which follows the physical intuition that those surfaces that more strongly bond with water, also more easily nucleate ice. Similar conclusions have been drawn from simulated Lennard-Jones systems, where the barrier to nucleation is found to decrease with an increasing strength of the surface interaction potential (Loeffler and Chen, 2013).

3.3 Contact parameter f

Unlike the binding energy, the geometric factor f cannot a priori be deduced and is therefore often treated as a fitting parameter. Following such a convention f can be considered to be single valued for individual substrates or some function of temperature $f \equiv f(T)$. In either case the observational data allow us to calculate individual values for each substrate at each temperature based on the measured S_i^{nuc} values.

The calculated f values serve as empirical fitting parameters for the observations, whose temperature dependence can be fitted using a least squares regression. Figures 5 and 6 show CNT solutions that demonstrate the temperature sensitivity of the f parameter, and the necessity of using a functional form at these temperatures. In Fig. 5 the experimental data is replotted with CNT solutions derived based on single f values determined for bare graphite. The theoretical curves demonstrate that with the correct choice of f individual data points can be modeled, but the trend with temperature deviates significantly from observations. At low temperatures the theory underpredicts S_i^{nuc} meaning nucleation is limited relative to the prediction, while at high temperatures, nucleation is enhanced (see Fig. 3 also). Thus, the observed nucleation behavior cannot be captured with the choice of a single-valued contact angle.

To capture the correct temperature trend it is necessary to assume a functional form $f(T)$. Examples of theoretical curves generated in this manner, using $f(T) = \exp(c_1 T) + c_2$ where c_1 and c_2 are constants produced by the least squares regressions done for each substrate material, are shown in Fig. 6. For each substrate the value of f decreases with increasing temperature, suggesting surfaces that are becoming more "wettable" in the traditional interpretation. The form of $f(T)$ is chosen to avoid the unphysical complication of a zero crossing that results from a simple linear fitting. However, within the experimental temperature range the details of the functional form have little effect on the global fitting. Thus, as expected Fig. 6 demonstrates that by combining the binding energy and a functional form of the geometric factor, CNT can be used to capture the observed behavior.

It is possible to proceed one step further and calculate a physical contact angle θ from $f(m) = (2+m)(1-m)^2/4$ where $m = \cos(\theta)$, which is an expression derived from purely geometrical considerations of a spherical nucleation

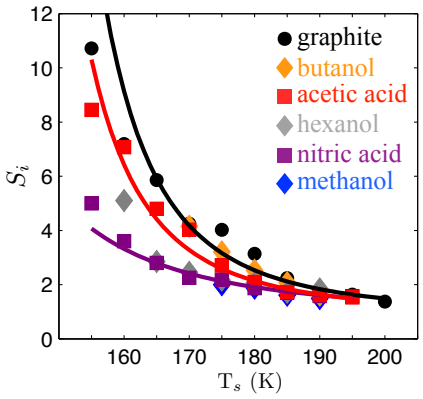

Figure 6. Measurement data plotted as in Fig. 2 with the CNT theoretical lines for the graphite (black), AcOH (red) and HNO_3 (violet) overlaid. The theoretical lines utilize least squares $f(T)$ fits to the calculated f parameters for each substrate, and illustrate the flexibility of this type of fitting – which performs equally well at the extrema of the measured data. However, the contact angles calculated from the $f(T)$ fits do not seem physically reasonable.

cap (cf. Turnbull and Vonnegut, 1952; Pruppacher and Klett, 1997). However, at these temperatures such a wholly geometric picture of the freezing nucleus is, in fact, unphysical and thus the resulting values for contact angle θ are not necessarily intuitive. For example, based on a least squares fitting of S_i^{nuc} for graphite, where $E_{ads} = 0.13$ eV, the f values range from 0.17 to 0.009 or $\theta \approx 61$–$27°$. In contrast the contact angle of water on graphite is expected to be between 80° and 90° (Adamson and Gast, 1997). Although, the hydrophilicity of graphite may certainly change with temperature and concentration of water molecules, there exists no straightforward method for asymptotically matching contact angles derived from nucleation experiments with contact angles measured using bulk materials at temperatures near or above the liquidous. Furthermore, even if the contact angle had a strong temperature dependence within a certain temperature range, there is no known physical reason why it would have a similar dependence irrespective of the underlying surface material. Hence, the origin of the strong temperature dependence is unlikely to be a result of a changing contact parameter.

Ultimately we are are left with a dilemma. Due to the nature of the system, the heterogeneous CNT treatment of the results presented here yields excellent theoretical fits to the data (Fig. 6) that remain to be explained physically (Sect. 4). Conversely, the results also appear to be well modeled empirically by a simple shift of the homogeneous nucleation curve (Fig. 3), which is difficult to explain for different reasons.

4 Discussion and atmospheric implications

The experimental results that we have presented demonstrate that at temperatures below 200 K high water vapor supersaturations are required to nucleate ice on substrate surfaces. Although the results can be replicated using the versatility of CNT, the theoretical results do not lend themselves to a ready physical explanation. From a theoretical standpoint, much of the unique behavior that seems to straddle the developed homogeneous and heterogeneous CNT can be reasonably explained by close examination of the underpinnings of the heterogeneous theory presented in Sect. 3.1 and by recognizing that there is an underlying strong pressure dependence on temperature. The ideal gas law and the Clausius–Clapeyron relation guarantee that as H_2O vapor becomes rarified supersaturations must increase to compensate for the decreasing pressure. In the present heterogeneous CNT model the term for monomer adsorption N_{ads} contains a strong temperature dependence that acts to mitigate the effect of increasing S. However, it does so in a manner that is overemphasized, because in its present form N_{ads} accounts only for pure monomolecular adsorption and desorption. In fact it is more likely that monomers adsorb and diffuse on the surface and thus interact with other monomers and molecular clusters, thereby depleting the effective monomer concentration and reducing the nucleation rate (Kroon and Ford, 2011). In lieu of a strict bookkeeping of the complicated molecular kinetics the heterogeneous CNT introduces f, which compensates for the strong thermal dependence in the binding energy term but does not comply with physical intuition. Thus, a more complete description of deposition nucleation from rarified gas is likely to be homologous with understanding thin-film nucleation, which explicitly reduces the dimensionality of the problem in the correct manner and eliminates geometric factors that are open to misinterpretation (Venables et al., 1984).

There are a number of other factors that also help to explain the difficulty of strict CNT treatments at these temperatures and encourage us to reexamine proposed alternatives for describing spontaneous nucleation. In a review of homogeneous nucleation Oxtoby (1992) gives a good summary of the shortcomings of, and myriad assumptions in CNT. In general the approximations of CNT, when considering nucleation as in this case forming solid from a dilute vapor where there exists a strong singularity in the density parameter at the phase boundary, are well controlled. However, at these experimental temperatures the critical cluster sizes that can be calculated vis-á-vis CNT are $\mathcal{O}(10)$ to $\mathcal{O}(100)$ molecules, and as a result the expected system behavior may not be consistent with what is predicted by bulk thermodynamics. The underlying question in nucleation, which remains open, is the applicability of macroscopic concepts to molecular-scale clusters (Oxtoby, 1992, 1999).

Kinetic theories of nucleation are an alternative to classical thermodynamic theories that have been developed (e.g., Katz and Spaepen, 1978). The kinetic approach relies on constraining the growth and decay of small clusters without relying on surface energies, which are measured macroscopic properties. Instead cluster growth and decay can be constrained by the interaction potential of the material, which

of course involves its own unique assumptions. Unfortunately, kinetic theories also have free parameters that must be constrained by comparison with experimental nucleation rates etc., and thus prevent strict first-principles calculations (Nowakowski and Ruckenstein, 1991). Perhaps the most well developed kinetic treatment is presented in a recent study by Kroon and Ford (2011) where they proffer a set of microscopic rate equations to describe cluster population dynamics. They explicitly include the contributions of both surface diffusion and direct deposition and although they find that for nanometer-scale atmospheric aerosols the diffusive flux will be small, it is clear that for large surfaces like those considered in the present study, surface diffusion may dominate clustering. The Kroon and Ford (2011) approach fundamentally agrees with the ideas of Venables et al. (1984) concerning thin film nucleation and growth. Venables et al. (1984) points out that while some parts of such processes may be in "local" equilibrium, nucleation and growth are fundamentally non-equilibrium phenomena. Thus, the detailed balance assumed when using the model of bulk thermodynamics may not exist everywhere. For example, kinetic limitations mean that crystals do not necessarily assume equilibrium geometries predicted by CNT. Thus, for nucleation, it appears crucial to maintain detailed molecular understanding of the clustering process until the clusters reach their critical size.

Kinetic theories also illustrate the importance of capturing the true interaction potentials in the system and thus hint that more complete theoretical approaches must utilize a theoretical skeleton that captures intermolecular interactions (Oxtoby, 1992). For example, density functional theory provides a non-classical approach whereby molecular scale effects can be preserved while employing mean density fields. Although density functional methods are fundamentally exact, real calculations require approximations that are subject to choices like the free-energy functional. Even so, such non-classical approaches can be used to calculate ΔG^* values that are augmented significantly from those of CNT. A higher nucleation barrier height ΔG^* results in significantly larger required undercooling or higher $S_{\mathrm{i}}^{\mathrm{nuc}}$ (cf. Fig. 4 in Oxtoby, 1992). Functionals that can be applied to nucleation are continually improving and should be tested for the systems we have probed experimentally.

In the context of other phase change phenomena involving H_2O, the strength and range of intermolecular interactions can strongly influence the character of the stable vs. metastable equilibrium. Premelting, which refers to the metastable disordering of ice layers as the melting temperature is approached, is an example of just such a phenomenon (Dash et al., 2006). In premelting theory liquid melt evolves from crystalline surfaces as temperature and impurity change in ways that depend sensitively on the magnitude and fall-off of the relevant intermolecular interactions (Wettlaufer, 1999; Thomson et al., 2010; Bartels-Rausch et al., 2014). Predicted sensitivities have been experimentally probed and observations confirm the basic theoretical assertions (Elbaum et al., 1993; Thomson et al., 2013). Although, the processes of nucleation and melting are not reversible, in both cases capturing the details requires an intimate understanding of the governing interactions.

The experimental observations that have been presented herein are most applicable to the coldest ice forming regions of the atmosphere. In the atmosphere ice nucleating substrates are in the form of small particles that are certainly different from the idealized macroscopic surfaces studied. It is well known that particle size and morphology can have an impact on the nucleating properties of atmospheric aerosols. In particular, particle shape or surface structure may alter the free energy landscape in a manner that promotes ice nucleation (Marcolli, 2014). That said, within our experimental range of temperature ≤ 200 K, the rarification of the vapor is likely to remain the leading order limitation on nucleation. In fact, as was previously discussed, at such temperatures the lack of a diffusive flux over small surfaces may act to further inhibit nucleation. This study is aimed at developing the molecular-level understanding of spontaneous nucleation and thus without further empirical evidence it is difficult to precisely predict the behavior of an analogous heterogeneous aerosol.

The observations do augment a small compendium of existing experimental deposition nucleation work that extends below 200 K. In the past this work has been motivated by studies of exoplanetary atmospheres like that of Mars, where temperatures are quite low but mineral dust and other aerosol particles may be abundant (e.g., Phebus et al., 2011; Cziczo et al., 2013). Trainer et al. (2009) and later Iraci et al. (2010) investigated deposition freezing on surrogate mineral dust materials. In both cases they discovered high requisite supersaturations, particularly for the limited measurements made below 170 K. Their analyses focused on using the empirically determined contact angle to parameterize the freezing and in the case of Trainer et al. (2009), they too observe a strong low-temperature dependence. However, once again the physical interpretation of the temperature dependence can only be described as the, "average surface activity" of the substrate material. Thus, the existing evidence serves to confirm the thesis that we are lacking a systematic microphysical understanding of low-temperature nucleation. Although we do not yet know how the low-temperature observations can be extrapolated to higher temperatures, it is clear that a successful theoretical treatment should capture observed behavior over the entire temperature range. Our analysis demonstrates the deftness of CNT, yet lays bare that what is missing is a physically descriptive theory with true predictive capabilities.

5 Conclusions

In this study we have presented results from deposition-mode ice nucleation on substrate surfaces at temperatures below

200 K. Previously, there have been limited observations of ice nucleation at these temperatures, and thus these results expand the breadth of materials studied under such conditions. Our observations are consistent with previous studies and both demonstrate the necessity of very high supersaturations to initiate ice nucleation at ≤ 200 K. Observed supersaturations far exceed predicted critical saturations that are based on macroscopic theories and extrapolations from solid and liquid properties at higher temperatures. Thus, the observations are indicative of an incomplete understanding of the key processes controlling systems under such conditions. Developing a better micro-physical understanding will have implications for how we understand nucleation in the atmosphere and more generally as a fundamental process important in many molecular systems.

An analysis of the experimental results based in CNT demonstrates that differences in the water adsorption energy on the different investigated substrate surfaces can partially but not completely explain the observed critical saturation ratios. Ice is observed to nucleate more easily on surfaces with larger H_2O affinities. To describe the sharp increase of S_i^{nuc} a temperature dependent contact parameter may be employed. For individual experiments the contact parameter can be determined explicitly, but a clear physical explanation for the parameter values is lacking. Due to its system specificity, this method of characterizing nucleation also suffers from limited predictive power.

Casting aside the issues of CNT, these new observations offer insight into the basic process of deposition nucleation. With the hope of robustly capturing such behavior, they also spur us to consider more detailed descriptions of the intermolecular interactions that lead from molecular clustering to nucleation. In addition to the development of more accurate theoretical models future work should focus on systematically determining the importance of material properties and detailed examinations of behavior at higher temperatures, where eventually macroscopic models will capture the system behavior.

Acknowledgements. This work is supported by the Swedish Research Council, and the Nordic Top-Level Research Initiative CRAICC. PP thanks the Wenner-Gren Foundation for providing funding for an extended stay at the University of Gothenburg. This work has benefited greatly from discussions with N. Marković.

Edited by: M. Boy

References

Adamson, A. and Gast, A.: Physical Chemistry of Surfaces, Wiley, New York, NY, 784 pp., 1997.

Allouche, A. and Bahr, S.: Acetic Acid–Water Interaction in Solid Interfaces, J. Phys. Chem. B, 110, 8640–8648, doi:10.1021/jp0559736, 2006.

Andersson, P. U., Suter, M. T., Marković, N., and Pettersson, J. B. C.: Water condensation on graphite studied by elastic helium scattering and molecular dynamics simulations, J. Phys. Chem. C, 111, 15258–15266, 2007.

Bartels-Rausch, T., Jacobi, H.-W., Kahan, T. F., Thomas, J. L., Thomson, E. S., Abbatt, J. P. D., Ammann, M., Blackford, J. R., Bluhm, H., Boxe, C., Domine, F., Frey, M. M., Gladich, I., Guzmán, M. I., Heger, D., Huthwelker, Th., Klán, P., Kuhs, W. F., Kuo, M. H., Maus, S., Moussa, S. G., McNeill, V. F., Newberg, J. T., Pettersson, J. B. C., Roeselová, M., and Sodeau, J. R.: A review of air-ice chemical and physical interactions (AICI): liquids, quasi-liquids, and solids in snow, Atmos. Chem. Phys., 14, 1587–1633, doi:10.5194/acp-14-1587-2014, 2014.

Chen, J.-P., Hazra, A., and Levin, Z.: Parameterizing ice nucleation rates using contact angle and activation energy derived from laboratory data, Atmos. Chem. Phys., 8, 7431–7449, doi:10.5194/acp-8-7431-2008, 2008.

Cziczo, D. J., Garimella, S., Raddatz, M., Hoehler, K., Schnaiter, M., Saathoff, H., Moehler, O., Abbatt, J. P. D., and Ladino, L. A.: Ice nucleation by surrogates of Martian mineral dust: What can we learn about Mars without leaving Earth?, J. Geophys. Res.-Planet., 118, 1945–1954, doi:10.1002/jgre.20155, 2013.

Dash, J. G., Rempel, A. W., and Wettlaufer, J. S.: The physics of premelted ice and its geophysical consequences, Rev. Mod. Phys., 78, 695–741, 2006.

Dymarska, M., Murray, B. J., Sun, L., Eastwood, M. L., Knopf, D. A., and Bertram, A. K.: Deposition ice nucleation on soot at temperatures relevant for the lower troposphere, J. Geophys. Res.-Atmos., 111, D04204, doi:10.1029/2005JD006627, 2006.

Elbaum, M., Lipson, S., and Dash, J.: Optical study of surface melting on ice, J. Cryst. Growth, 129, 491–505, 1993.

Fletcher, N. H.: Size Effect in Heterogeneous Nucleation, J. Chem. Phys., 29, 572–576, doi:10.1063/1.1744540, 1958.

Fortin, T. J., Drdla, K., Iraci, L. T., and Tolbert, M. A.: Ice condensation on sulfuric acid tetrahydrate: Implications for polar stratospheric ice clouds, Atmos. Chem. Phys., 3, 987–997, doi:10.5194/acp-3-987-2003, 2003.

Girshick, S. L. and Chiu, C.: Kinetic nucleation theory: A new expression for the rate of homogeneous nucleation from an ideal supersaturated vapor, J. Chem. Phys., 93, 1273–1277, doi:10.1063/1.459191, 1990.

Hale, B. N. and Plummer, P. L. M.: Molecular model for ice clusters in a supersaturated vapor, J. Chem. Phys., 61, 4012–4019, doi:10.1063/1.1681694, 1974.

Hoose, C. and Möhler, O.: Heterogeneous ice nucleation on atmospheric aerosols: a review of results from laboratory experiments, Atmos. Chem. Phys., 12, 9817–9854, doi:10.5194/acp-12-9817-2012, 2012.

Hoose, C., Kristjansson, J. E., Chen, J.-P., and Hazra, A.: A Classical-Theory-Based Parameterization of Heterogeneous Ice Nucleation by Mineral Dust, Soot, and Biological Particles in a Global Climate Model, J. Atmos. Sci., 67, 2483–2503, doi:10.1175/2010JAS3425.1, 2010.

Iraci, L. T., Phebus, B. D., Stone, B. M., and Colaprete, A.: Water ice cloud formation on Mars is more difficult than presumed: Laboratory studies of ice nucleation on surrogate ma-

terials, Icarus, 210, 985–991, doi:10.1016/j.icarus.2010.07.020, 2010.

Kashchiev, D.: Nucleation: Basic Theory with Applications, Butterworth-Heinemann, Oxford, 544 pp., 2000.

Kashchiev, D.: Analysis of experimental data for the nucleation rate of water droplets, J. Chem. Phys., 125, 044505, doi:10.1063/1.2222373, 2006.

Katz, J. L. and Spaepen, F.: A kinetic approach to nucleation in condensed systems, Philosophical Magazine Part B, 37, 137–148, doi:10.1080/01418637808226648, 1978.

Knopf, D. A. and Koop, T.: Heterogeneous nucleation of ice on surrogates of mineral dust, J. Geophys. Res.-Atmos., 111, D12201, doi:10.1029/2005JD006894, 2006.

Kołaski, M., Zakharenko, A. A., Karthikeyan, S., and Kim, K. S.: Structures, Energetics, and IR Spectra of Monohydrated Inorganic Acids: Ab initio and DFT Study, J. Chem. Theory Comput., 7, 3447–3459, doi:10.1021/ct100428z, 2011.

Kong, X., Andersson, P. U., Marković, N., and Pettersson, J. B. C.: Environmental Molecular Beam Studies of Ice Surface Processes, in: Physics and Chemistry of Ice 2010, edited by: Furukawa, Y., Sazaki, G., Uchida, T., and Watanabe, N., 79–88, Hokkaido University Press, Sapporo, Japan, 2011.

Kong, X., Andersson, P. U., Thomson, E. S., and Pettersson, J. B. C.: Ice Formation via Deposition Mode Nucleation on Bare and Alcohol-Covered Graphite Surfaces, J. Phys. Chem. C, 116, 8964–8974, doi:10.1021/jp212235p, 2012.

Kong, X., Thomson, E. S., Papagiannakopoulos, P., Johansson, S. M., and Pettersson, J. B. C.: Water accommodation on ice and organic surfaces: Insights from environmental molecular beam experiments, J. Phys. Chem. B, 118, 13378–13386, 2014.

Koop, T., Luo, B. P., Tsias, A., and Peter, T.: Water activity as the determinant for homogeneous ice nucleation in aqueous solutions, Nature, 406, 611–614, 2000.

Kroon, C. M. L.-V., and Ford, I. J.: Becker–Döring rate equations for heterogeneous nucleation, with direct vapour deposition and surface diffusion mechanisms, Atmos. Res., 101, 553–561, doi:10.1016/j.atmosres.2010.12.019, 2011.

Lakhlifi, A. and Killingbeck, J. P.: Investigation of the interaction of some astrobiological molecules with the surface of a graphite (0 0 0 1) substrate. Application to the CO, HCN, H_2O and H_2CO molecules, Surface Science, 604, 38–46, doi:10.1016/j.susc.2009.10.017, 2010.

Liu, X. Y.: A new kinetic model for three-dimensional heterogeneous nucleation, J. Chem. Phys., 111, 1628–1635, doi:10.1063/1.479391, 1999.

Loeffler, T. D. and Chen, B.: Surface induced nucleation of a Lennard-Jones system on an implicit surface at sub-freezing temperatures: A comparison with the classical nucleation theory, J. Chem. Phys., 139, 234707, doi:10.1063/1.4848737, 2013.

Marcolli, C., Gedamke, S., Peter, T., and Zobrist, B.: Efficiency of immersion mode ice nucleation on surrogates of mineral dust, Atmos. Chem. Phys., 7, 5081–5091, doi:10.5194/acp-7-5081-2007, 2007.

Marcolli, C.: Deposition nucleation viewed as homogeneous or immersion freezing in pores and cavities, Atmos. Chem. Phys., 14, 2071–2104, doi:10.5194/acp-14-2071-2014, 2014.

Marković, N., Andersson, P. U., Någård, M. B., and Pettersson, J. B. C.: Scattering of water from graphite: simulations and experiments, Chemical Physics, 247, 413–430, doi:10.1016/S0301-0104(99)00324-9, 1999.

Möhler, O., Buttner, S., Linke, C., Schnaiter, M., Saathoff, H., Stetzer, O., Wagner, R., Kramer, M., Mangold, A., Ebert, V., and Schurath, U.: Effect of sulfuric acid coating on heterogeneous ice nucleation by soot aerosol particles, J. Geophys. Res.-Atmos., 110, D11210, doi:10.1029/2004JD005169, 2005.

Möhler, O., Field, P. R., Connolly, P., Benz, S., Saathoff, H., Schnaiter, M., Wagner, R., Cotton, R., Krämer, M., Mangold, A., and Heymsfield, A. J.: Efficiency of the deposition mode ice nucleation on mineral dust particles, Atmos. Chem. Phys., 6, 3007–3021, doi:10.5194/acp-6-3007-2006, 2006.

Murphy, D. M. and Koop, T.: Review of the vapour pressures of ice and supercooled water for atmospheric applications, Q. J. Roy. Meteor. Soc., 131, 1539–1565, doi:10.1256/qj.04.94, 2005.

Murray, B. J. and Jensen, E. J.: Homogeneous nucleation of amorphous solid water particles in the upper mesosphere, J. Atmos. Sol.-Terr. Phy., 72, 51–61, doi:10.1016/j.jastp.2009.10.007, 2010.

Niedermeier, D., Shaw, R. A., Hartmann, S., Wex, H., Clauss, T., Voigtländer, J., and Stratmann, F.: Heterogeneous ice nucleation: exploring the transition from stochastic to singular freezing behavior, Atmos. Chem. Phys., 11, 8767–8775, doi:10.5194/acp-11-8767-2011, 2011.

Nowakowski, B. and Ruckenstein, E.: A kinetic approach to the theory of nucleation in gases, J. Chem. Phys., 94, 1397–1402, doi:10.1063/1.459997, 1991.

Oxtoby, D. W.: Homogeneous nucleation: theory and experiment, Journal of Physics: Condensed Matter, 4, 7627, doi:10.1088/0953-8984/4/38/001, 1992.

Oxtoby, D. W.: Nucleation and Surface Melting of Ice, in: Ice Physics and the Natural Environment, edited by: Wettlaufer, J., Dash, J., and Untersteiner, N., vol. 56 of NATO ASI Series, Springer, Berlin Heidelberg, 23–38, doi:10.1007/978-3-642-60030-2_3, 1999.

Papagiannakopoulos, P., Kong, X., Thomson, E. S., Marković, N., and Pettersson, J. B. C.: Surface Transformations and Water Uptake on Liquid and Solid Butanol near the Melting Temperature, J. Phys. Chem. C, 117, 6678–6685, doi:10.1021/jp4003627, 2013.

Papagiannakopoulos, P., Kong, X., Thomson, E. S., and Pettersson, J. B. C.: Water Interactions with Acetic Acid Layers on Ice and Graphite, J. Phys. Chem. B, doi:10.1021/jp503552w, 2014.

Phebus, B. D., Johnson, A. V., Mar, B., Stone, B. M., Colaprete, A., and Iraci, L. T.: Water ice nucleation characteristics of JSC Mars-1 regolith simulant under simulated Martian atmospheric conditions, J. Geophys. Res.-Planet., 116, E04009, doi:10.1029/2010JE003699, 2011.

Pratte, P., van den Bergh, H., and Rossi, M. J.: The kinetics of H_2O vapor condensation and evaporation on different types of ice in the range 130–210 K, J. Phys. Chem. A, 110, 3042–3058, doi:10.1021/jp053974s, 2006.

Pruppacher, H. R. and Klett, J. D.: Microphysics of Coulds and Precipitation, 2nd edn., Kluwer Academic Publ., Dordrecht, the Netherlands, 954 pp., 1997.

Rubeš, M., Nachtigall, P., Vondrášek, J., and Bludský, O.: Structure and stability of the water–graphite complexes, J. Phys. Chem. C, 113, 8412–8419, doi:10.1021/jp901410m, 2009.

Shilling, J. E., Fortin, T. J., and Tolbert, M. A.: Depositional ice nucleation on crystalline organic and inorganic solids, J. Geophys. Res.-Atmos., 111, D12204, doi:10.1029/2005JD006664, 2006.

Staikova, M. and Donaldson, D. J.: Ab initio investigation of water complexes of some atmospherically important acids: HONO, HNO_3 and HO_2NO_2, Phys. Chem. Chem. Phys., 3, 1999–2006, doi:10.1039/B101755L, 2001.

Tao, F.-M., Higgins, K., Klemperer, W., and Nelson, D. D.: Structure, binding energy, and equilibrium constant of the nitric acid-water complex, Geophys. Res. Lett., 23, 1797–1800, doi:10.1029/96GL00947, 1996.

Thomson, E. S., Benatov, L., and Wettlaufer, J. S.: Erratum: Abrupt grain boundary melting in ice [Phys. Rev. E 70, 061606 (2004)], Phys. Rev. E, 82, 039907, doi:10.1103/PhysRevE.82.039907, 2010.

Thomson, E. S., Kong, X., Andersson, P. U., Marković, N., and Pettersson, J. B. C.: Collision dynamics and solvation of water molecules in a liquid methanol film, J. Phys. Chem. Lett., 2, 2174–2178, doi:10.1021/jz200929y, 2011.

Thomson, E. S., Hansen-Goos, H., Wettlaufer, J. S., and Wilen, L. A.: Grain boundary melting in ice, J. Chem. Phys., 138, 124707, doi:10.1063/1.4797468, 2013.

Trainer, M. G., Toon, O. B., and Tolbert, M. A.: Measurements of depositional ice nucleation on insoluble substrates at low temperatures: implications for Earth and Mars, J. Phys. Chem. C, 113, 2036–2040, doi:10.1021/jp805140p, 2009.

Turnbull, D. and Vonnegut, B.: Nucleation Catalysis, Ind. Eng. Chem., 44, 1292–1298, doi:10.1021/ie50510a031, 1952.

Venables, J. A., Spiller, G. D. T., and Hanbucken, M.: Nucleation and Growth of Thin-Films, Rep. Prog. Phys., 47, 399–459, 1984.

Voloshina, E., Usvyat, D., Schutz, M., Dedkov, Y., and Paulus, B.: On the physisorption of water on graphene: a CCSD(T) study, Phys. Chem. Chem. Phys., 13, 12041–12047, doi:10.1039/C1CP20609E, 2011.

Wettlaufer, J. S.: Impurity effects in the premelting of ice, Phys. Rev. Lett., 82, 2516–2519, 1999.

Winkler, P. M., Steiner, G., Vrtala, A., Vehkamäki, H., Noppel, M., Lehtinen, K. E. J., Reischl, G. P., Wagner, P. E., and Kulmala, M.: Heterogeneous nucleation experiments bridging the scale from molecular ion clusters to nanoparticles, Science, 319, 1374–1377, 2008.